Asian Journal of Chemistry; Vol. 26, No. 5 (2014), 1257-1260

ASIAN JOURNAL OF CHEMISTRY

http://dx.doi.org/10.14233/ajchem.2014.17201

Synthesis and Optical Property of ZnO/SiO_2 Nanocomposite Cryogels†

LIFEN SU[1], LEI MIAO[2,*], MING ZHANG[3], JIASHENG QIAN[1], RU XIA[1], BIN YANG[1] and PENG CHEN[1]

[1]Anhui Province Key Laboratory of Environment-Friendly Polymer Materials, College of Chemistry and Chemical Engineering, Anhui University, Hefei 230601, P.R. China
[2]Key Laboratory of Renewable Energy, Guangzhou Institute of Energy Conversion, Chinese Academy of Sciences, Guangzhou 510640, P.R. China
[3]Department of Physics, Graduate School of Engineering, Yokohama National University,Yokohama 240-8501, Japan

*Corresponding author: Fax: +86 551 63861480; E-mail: ausulf@sina.com; Fax: +86 20 87035351; E-mail: maiolei@ms.giec.ac.cn

Published online: 1 March 2014; AJC-14742

In this paper, ZnO cryogels with a dopant of SiO_2 with molar ratio of 9:1 to 1:1 were prepared by sol-gel technology and dried by a novel vacuum freeze drying using a co-precursor method. The as-prepared ZnO/SiO_2 nanocomposites were annealed in air at 250, 500 and 800 ºC for 45 min, respectively. The structure and morphology of the nanocomposites were determined by X-ray diffraction (XRD) and field emission scanning electron microscopy. The optical properties were estimated not only by UV-visible spectrometer but also theoretical calculation. The annealed nanocomposites exhibited hexagonal Wurtzite structure ZnO and whose crystallinity became better as an increase of annealing temperature. The amounts of doping SiO_2 affect the optical band gaps and morphology of ZnO/SiO_2 nanocomposites significantly. After annealing, the obtained ZnO nanorods grow up in size from the SEM images with annealing temperature ranging from 250 to 500 ºC and flowerlike ZnO was formed with tetragonal pillars at 800 ºC.

Keywords: Optical band gap, ZnO/SiO_2 nanocomposites, Cryogels, Co-precursor method.

INTRODUCTION

Zinc oxide is a hot semiconductor material due to its unique electronic, optical and acoustical properties[1-6]. ZnO-based composites are of considerable interest in ceramics technology[7] for applications as sensors, semiconductor devices and varistors[8], which usually call for smaller especially nanoscale particles with special morphology. In order to control particle sizes and their distributions of the composites, silicon dioxide is popular as host matrices[9] for insertion of ZnO nanoparticles due to its unique properties[10]. The ZnO/SiO_2 films have received lots of attention because of their particular applications as luminescent materials[11,12] and gas sensors[13]. In addition, most of the reported ZnO/SiO_2 core/shell composites were usually prepared by hydrothermal[14] and atomic-layer deposition (ALD) methods[15]. However, these processes are too expensive and unwanted reactions between nanoparticles and silica matrix occurred during temperature treatments from 500 ºC onwards because of the depolymerization of host matrix[16]. Recently, Anedda *et al.*[16] and Cui *et al.*[17] have reported a new sol-gel route by using a self-combusion and epoxide-assisted process to prepare ultrafine ZnO/SiO_2 composites. Up to now, the works of finding a low-cost approach and controlling the shape, size and properties of the ZnO/SiO_2 nanocomposites are still under way for researchers.

In the present study, the low-cost sol-gel technology followed by a novel vacuum freeze drying[18] using a co-precursor method was utilized to prepare the ZnO/SiO_2 nanocpmposites in a simpler way. The structural and optical properties of the obtained ZnO/SiO_2 nanocomposites are investigated by both experimental and calculational methods.

EXPERIMENTAL

The chemicals used for the preparation of alcogels were tetraethoxysilane (TEOS, $SiO_2 \geq 28.5$ %), zinc acetate [$Zn(CH_3COO)_2 \cdot 2H_2O$, 99 %], acetic acid (99.5 %), *tert*-butyl alcohol (TBA, 99 %), hydrochloric acid (36.5 %) and ammonia (28 %) were purchased from Aladdin Reagent Database Inc. (China). The double distilled water was prepared in the authors laboratory.

The wet gels were synthesized *via* a sol-gel technology using co-precursor method as reported[19]. In the case of ZnO

†Presented at The 7th International Conference on Multi-functional Materials and Applications, held on 22-24 November 2013, Anhui University of Science & Technology, Huainan, Anhui Province, P.R. China

precursor solution, $Zn(CH_3COO)_2{\cdot}2H_2O$ was added to distilled water and acetic acid was added as a catalyst then the mixed solution was vigorously stirred for 3 h at 60 ºC. The molar ratio of $Zn(CH_3COO)_2{\cdot}2H_2O$:$H_2O$:acetic acid were taken as $1:40:1.0 \times 10^{-3}$. Then for the SiO_2 solution, tetraethoxysilane, *tert*-butyl alcohol, H_2O with appropriate HCl was mixed under continuous stirring for complete hydrolysis with molar ratio at $1:7:3.7:5.7 \times 10^{-3}$. In order to get the ZnO/SiO_2 wet gels, the obtained solutions were mixed under constant stirring for 10 min with calculated amounts, followed by the addition of ammonia (NH_4OH) catalysis for condensation. The alcosols were then transferred to a culture dish and gelled. The gels were dried by a vacuum freeze dryer (Christ Alpha 2-4 LSC, Germany). Finally, the obtained cryogels were annealed at 250, 500 and 800 ºC for 45 min, respectively.

The crystallizing nature of the nanocomposite powders was examined by X-ray diffraction (XRD, X'Pert Pro MPD/PW3040/60, Holland). The absorbance spetra of the nanocomposites were measured by a UV/VIS spectrometer (Lambda 750, Perkin Elmer, USA). The calculation of energy gap was carried out by using the software of CASTEP (Cambridge Serial Total Energy Package)[20]. The microstructure of the ZnO/SiO_2 nanocomposites was observed by a Field Emission Scanning Electron Microscopy (FE-SEM, Hitachi S-4800, Japan).

RESULTS AND DISCUSSION

The XRD patterns of ZnO/SiO_2 nanocomposites with different molar ratio and annealing temperature are shown in Fig. 1. They all exhibited hexagonal wurtzite structure of ZnO (JCPDS 36-1451) which are in good agreement with the previous result[3] and no indication of a phase SiO_2 is found. The peak intensities of the composites annealed at 250 ºC become weaker with more content of dopant SiO_2, which indicate that SiO_2 has been successfully doped into the ZnO lattice and thus the weakened peaks occur. Compared with the full width at half maximum (FWHM) for (101) peaks in Fig. 1, it can be observed that the crystallinity of ZnO tends to be better with less dopant SiO_2 and an increasing annealing temperture. This is due to that higher temperature can contribute to the growth of ZnO crystallinity. When the annealing temperture is higher than 500 ºC, the improvement of crystallinity is very little.

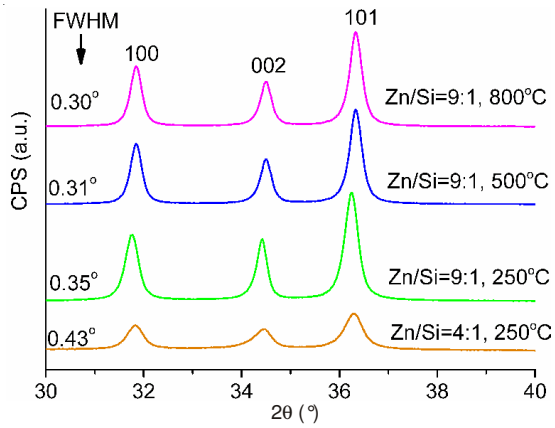

Fig. 1. XRD patterns of ZnO/SiO_2 nanocomposites with different molar ratio and the values of FWHMs for (101) peaks

The effect of SiO_2 doping concentration on the optical band gap of ZnO was further investigated by UV-visible absorption spectroscopy. Fig. 2 shows the absorbance of ZnO/SiO_2 nanocomposites annealed at 250 ºC with different molar ratio. A red shift was observed in absorption band edge of the nanocomposites with an increasing dopant of SiO_2, which may be ascribed to the incorporation of SiO_2 inside ZnO lattice. It is also observed that two peaks exist at 400 nm (3.1 eV) and 220 nm (5.6 eV) due to ZnO and SiO_2, respectively. The coexisting peaks reveal that most of the ZnO/SiO_2 cryogels are compounds. The optical band gaps of ZnO and SiO_2 are known as 3.4 and 9.0 eV, respectively. However, the peaks at 220 nm become stronger and the optical band gap tends to be that of SiO_2 with an increase of dopant SiO_2. The photon energy of the peak value observed on the absorbance deviates apparently from the corresponding optical band gap of pure ZnO and SiO_2. These indicates that Si atom inserts the ZnO lattice leading to lower optical band gap of ZnO and similarly Zn atom dopes into the SiO_2 system resulting in lower optical band gap of SiO_2.

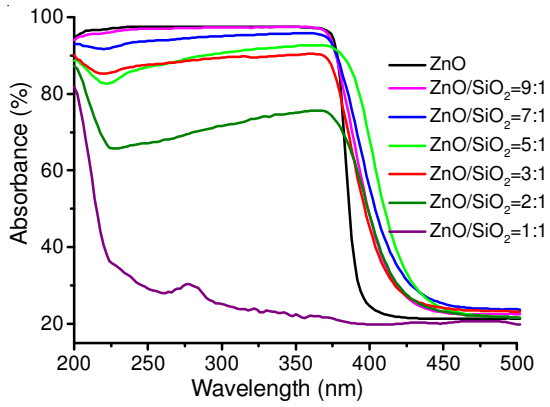

Fig. 2. Absorbance of ZnO/SiO_2 nanocomposites annealed at 250 ºC with different molar ratio

The first-principle pseudopotential method based on the density-functional theory (DFT)[21] was utilized to study the effect of different molar ratio of ZnO/SiO_2 on the optical band gap by investigating the electron structure of the nanocomposites. The ultrasoft pesudopotential generated by the scheme of Vanderbilt[22] was applied in this calculation. As for the method of approximation of the exchange-correlation term of the DFT, local density approximation (LDA) was used. Pseudo atomic calculation for O ($2s^2 2p^4$), Si ($3s^2 3p^2$), Zn ($3d^{10} 4s^2$), was performed. The local density approximation calculation is likely to give a narrower band gap than that of the observed result. Therefore, the band gap is adjusted to account for the scissors correction.

The Fermi level is set to be 0 eV and other energy levels are determined by comparing with Fermi level. The calculated densities of states have been shown in Fig. 3. It is obvious that the 3*s* and 3*p* orbitals of Si have been formed the impurity energy level in the case of Si doping into ZnO, which leads to the decrease of the energy gap of ZnO. While in the case of Zn incorporating into SiO_2, the impurity energy level was derived from the 3*d* orbital of Zn, which results in lower energy gap of SiO_2.

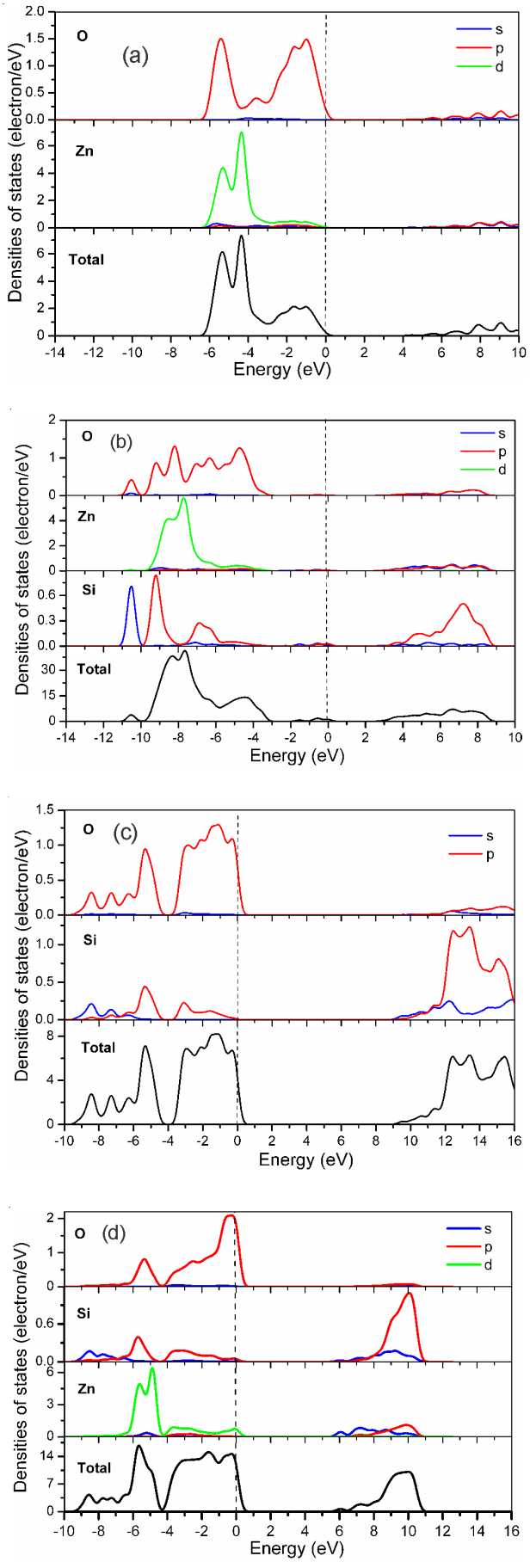

Fig. 3. Calculated densities of states: (a) pure ZnO, (b) Si doping ZnO, Zn/Si = 7, (c) pure SiO_2 and (d) Zn doping SiO_2, Si/Zn = 5

The absorption coefficient and the band gap energy can be calculated by eqn. 1[23].

$$\alpha h\gamma = A(h\gamma - E_g)^{1/2} \quad (1)$$

where hγ is the incident photon energy, E_g is the band gap energy and A is a constant. Fig. 4 shows the relation of calculational and experimental data of energy gap derived from different molar ratio of Zn/Si. Obviously, the theoretically calculated values of energy gaps are in good agreement with those of experiments. Therefore, the dopant of SiO_2 plays an important role on the optical band gap of ZnO/SiO_2 nanocomposites.

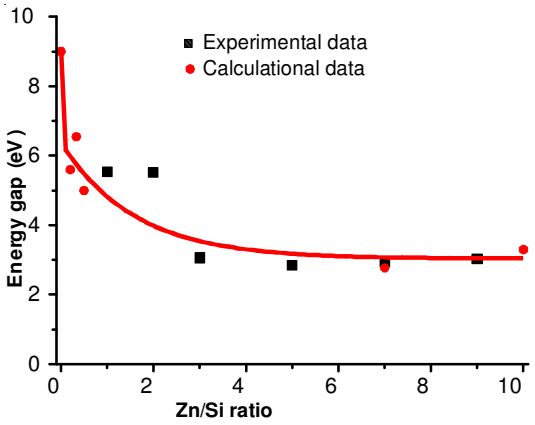

Fig. 4. Relation between experimental and calculational data of energy gap derived from different molar ratio of Zn/Si. The red line is the ExpGro 2 fit of the calculational data

The SEM images of ZnO/SiO_2 = 9:1 nanocomposites annealed at different temperature are shown in Fig. 5. The annealing temperature affects the morphology of the nanocomposites significantly. The doping SiO_2 grains like spheres are embedded in large ZnO nanorods lying with irregular directions. The ZnO nanorods grow up in size as the annealing temperature increase from 250 to 500 ºC. However, at 800 ºC, flowerlike Wurtzite ZnO with special tetragonal pillars centering to one point were formed, which are different from the ZnO morphology[24,25] may be ascribed to the novel synthesis and drying method of the study.

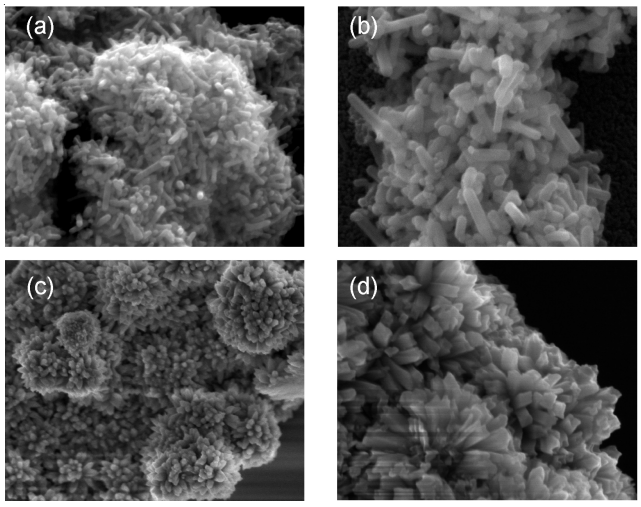

Fig. 5. (a), (b) and (c) are the SEM images of ZnO/SiO_2 = 9:1 annealed at: 250 °C, 500 °C and 800 ºC, respectively. (d) is the magnified SEM image in (c)

Conclusion

ZnO/SiO_2 nanocomposites are successfully fabricated by a low-cost co-precursor method followed by vacuum freeze drying. The experimental and calculational results show that the optical properties of the nanocomposites were affected by the dopant of SiO_2. The ZnO nanorods grow up in size as an increase of the annealing temperature from 250 to 500 ºC. However, a flowerlike Wurtzite ZnO sample with special tetragonal pillars can be formed at 800 ºC. These ZnO/SiO_2 nanocomposites will open up its applications in nanoelectronic device, catalysis, drug delivery system and sensor.

ACKNOWLEDGEMENTS

This work was financially supported by Anhui University Doctoral Scientific Research Funds 02303319.

REFERENCES

1. J. Zhang, L.D. Sun, J.L. Yin, H.L. Su, C.S. Liao and C.H. Yan, *Chem. Mater*., **14**, 4172 (2002).
2. J.M. Wang and L. Gao, *J. Mater. Chem*., **13**, 2551 (2003).
3. Z. Gui, J. Liu, Z.Z. Wang, L. Song, Y. Hu, W.C. Fan and D.Y. Chen, *J. Phys. Chem. B*, **109**, 1113 (2005).
4. L. Guo, Y.L. Ji, H. Xu, P. Simon and Z. Wu, *J. Am. Chem. Soc*., **124**, 14864 (2002).
5. D. Ledwith, S.C. Pillai, G.W. Watson and J.M. Kelly, *Chem. Commun.*, **20**, 2294 (2004).
6. J.H. Park, H.J. Choi, Y.J. Choi, S.H. Sohn and J.G. Park, *J. Mater. Chem*., **14**, 35 (2004).
7. S. Lu, H. Liu, L. Zhang and X. Yao, *Chin. Sci. Bull*., **41**, 230 (1996).
8. E.A. Abel-Aal, A.A. Ismail, M.M. Rashad and H. El-Shall, *J. Non-Cryst. Solids*, **352**, 399 (2006).
9. R. Moleski, E. Leontidis and F. Krumeich, *J. Colloid Interf. Sci*., **302**, 246 (2006).
10. K. Kanamori, *J. Ceram. Soc. Jpn*., **119**, 16 (2011).
11. S. Chakrabarti, D. Ganguli and S. Chaudhuri, *Phys. Status Solidi A*, **201**, 2134 ((2004).
12. W.C. Chen, *Mater. Lett*., **59**, 1239 (2005).
13. V. Musat, E. Fortunato, S. Petrescu and A.M. Botelho do Rego, *Phys. Status Solidi A*, **205**, 2075 (2008).
14. F. Li, X. Huang, Y. Jiang, L. Liu and Z. Li, *Mater. Res. Bull*., **44**, 437 (2009).
15. J. Hwang, B. Min, J.S. Lee, K. Keem, K. Cho, M.Y. Sung, M.S. Lee and S. Kim, *Adv. Mater*., **16**, 422 (2004).
16. R. Anedda, C. Cannas, A. Musinu, G. Pinna, G. Piccaluga and M. Casu, *J. Nanopart. Res*., **10**, 107 (2008).
17. H. Cui, M. Zayat and D. Levy, *J. Alloys Comp*., **474**, 292 (2009).
18. L.F. Su, L. Miao, G. Xu and S. Tanemura, *Adv. Mater. Res*., **105**, 852 (2010).
19. L.F. Su, L. Miao and S. Tanemura, *Mater. Sci. Forum*, **663-665**, 1242 (2010).
20. M.C. Payne, T.A. Arias and J.D. Joannopoulos, *Rev. Mod. Phys*., **64**, 1045 (1992).
21. W. Kohn and L.J. Sham, *Phys. Rev*., **140(4A)**, A1133 (1965).
22. D. Vanderbilt, *Phys. Rev. B*, **41**, 7892 (1990).
23. R. Elilarassi and G. Chandrasekaran, *J. Mater. Sci. Mater. Electron*., **22**, 751 (2011).
24. K. Han, Z. Zhao, Z. Xiang, C. Wang, J. Zhang and B. Yang, *Mater. Lett*., **61**, 363 (2007).
25. S. Chakraborty, A.K. Kole and P. Kumbhakar, *Mater. Lett.*, **67**, 362 (2012).